5-2013

Synthesis of Porphyrin and Porphyrinoid Structures for use in Binary Cancer Therapies: Fluorinated Porphyrin-Carborane as a candidate for Boron Neutron Capture Therapy and Tetrabenzoporphyrin with Polyamine Conjugates as a candidate for Photodynamic Therapy

Laura A. Clesi

Synthesis of Porphyrin and Porphyrinoid Structures for use in Binary Cancer Therapies:
Fluorinated Porphyrin-Carborane as a candidate for Boron Neutron Capture Therapy and Tetrabenzoporphyrin with Polyamine Conjugates as a candidate for Photodynamic Therapy

by

Laura A. Clesi

Undergraduate honors thesis under the direction of

Dr. M. Graca H. Vicente

Department of Chemistry

Submitted to the LSU Honors College in partial fulfillment of
the Upper Division Honors Program.

May 2013

Louisiana State University
& Agricultural and Mechanical College
Baton Rouge, Louisiana

Acknowledgements

Many thanks are due to both my graduate mentor Dinesh Bhupathiraju and my faculty advisor M. Graça H. Vicente for their direction and encouragement throughout the last year. Also, thanks are due to LSU and NSF for their funding and facilities and to Dr. Kresimir Rupnik and Dr. Granger Babcock for volunteering their time to evaluate this project.

Table of Contents

Abstract

It has long been established that porphyrins have the ability to selectively accumulate within tumor tissue, as well as having certain photosensitizing properties. A compound with these characteristics has great potential for use in two binary cancer therapy methods which minimalize the devastating side effects of conventional cancer therapies (i.e. surgery and chemotherapy); namely, Boron Neutron Capture Therapy (BNCT), which destroys tumor cells via ionization processes, and Photodynamic Therapy (PDT), which locally controls tumor eradication via a photosensitizer, oxygen, and light.

A series of three carborane-porphyrins has been synthesized in order to search for a more efficient drug to be used in BNCT. The fluorescent properties of the porphyrin allow the drug to be tracked as it travels throughout the body, while the caged structure of the carborane enhances the stability of the compound compared to other boron clusters as well as allows for high boron content. Based on these properties, a fluorinated carborane-porphyrin with a self-enhanced peptide conjugate was proposed as a potential solution.

In order to modify the porphyrin structure to enhance its potential for PDT, certain porphyrinoid candidates have been modified in order to shift absorbance to the near-IR range and increase cellular uptake even further by enhancing π-conjugation and synthesizing additional polyamine substituents, respectively. Such modifications have led to very promising results according to *in vitro* studies and toxicity tests, which reported low dark toxicity as well as high photo-toxicity during exposure to light. In

order to enhance these promising characteristics, this study focuses on the development of di-substituted porphyrinoid isomers with polyamine conjugates.

Ch. 1: Introduction

Conventional cancer therapies rely on removing or destroying diseased tissue, usually with invasive surgery or chemotherapy, and almost always with devastating side effects. In the continuing search to find an alternative treatment method that minimalizes these effects, much attention has been paid to two promising techniques already in clinical trials called boron neutron capture therapy (BNCT) and photodynamic therapy (PDT).

1.1 BNCT

BNCT is a therapeutic technique that is a possible treatment for brain tumors. The mechanism of how this technique occurs is represented by the following equation[1-3]:

$$^{10}B + {}^{1}n \rightarrow {}^{4}He^{2+} + {}^{7}Li^{3+} + \gamma + 2.4MeV$$

As the ^{10}B-containing drug preferentially accumulates within tumor cells, it is exposed to a low energy neutron beam, capturing the low energy neutrons and producing alpha particles ($^{4}He^{2+}$), Li ions, gamma rays, and 2.4 MeV of energy represented by MeV. These high linear energy transfer, or high-LET, particles (referring to the alpha and lithium particles) destroy tumor cells through ionization processes. During *in vivo* studies, high-LET α transmitters have been shown to be more effective than β emitters in the radioimunotherapy of solid tumors: at equitoxic dosing, metastatic models show a 95% cure rate in mice with high-LET particles compared to a 20% cure rate in mice utilizing low-LET (β) particles.[4] Because of the short path of high-LET particles in tissue due to the short half-life of radioisotopes such as the fast-clearing ^{4}He, the destructive effects are highly localized to ^{10}B-containing cells while neighboring healthy cells are not damaged. Also, ~ 10-30 μg of ^{10}B is needed per 1g of tumor, depending on

the location of the ^{10}B within the tumor cell. And while a high neutron beam would be toxic, the low neutron beam and gamma rays present in this process won't damage healthy human brain cells, as is shown by its low toxicity levels.

1.2 Current Clinical Trials for BNCT

Two compounds, 4-dihydroxyborylphenylalanine (BPA) and disodium-mercapto-closo-dodecarborate (BSH), are compounds in clinical trials as possible candidates for BNCT, each with certain areas that could be improved upon in an ideal drug for this therapeutic technique. Figure 1.1 below shows the structure of each compound.[5] BPA has low boron content which makes a large quantity of the drug necessary: about one mg per kg of body mass. BSH has high boron content, but low stability, as it often forms a dimerization bridge due to its –SH substituent. Also, both BPA and BSH have limited tumor selectivity. Our hope is to rectify these problems with the proposed fluorinated carborane porphyrin compound.

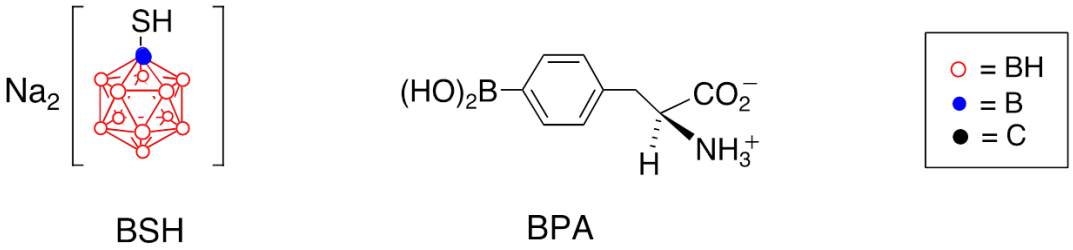

Figure 1.1. Structures of two current clinical trials, BSH and BPA.

1.3 Porphyrins

The word "porphyrin" is derived from the Greek "πορφύρα" meaning purple.[6] Porphyrins act as brightly colored chromophores due to their extensive π-conjugation system. Also due to a transition to the S2 state, a large band appears in UV-Vis spectra

called the Soret band,[6] which is discussed later in Chapter 3.3. Porphyrins have much higher tumor selectivity than these compounds currently in clinical trials and allow the compound to be tracked via fluorescence. Porphyrins also have several distinct sites such as the meso and β positions and hydrogens on the inner rings (as shown in Figure 1.2) which allow this structure to easily be modified for the addition of various functional groups in order to increase tumor selectivity or in hopes of making it easier for the compound to effectively cross the blood brain barrier (BBB). In continuance with the effort to bypass the BBB obstacle, our compound is neutral, which contrasts with the previously studied cobaltacarborane-porphyrin^{3-} and the tetrakis(p-carboranylthio-tetrafluorophenyl)chlorin or TPFC^{4-}.[7,8] The neutral compound is desired in order to make the drug more attractive to the membranes of neurological cells, which are negatively charged due to their phosphate groups. We are particularly interested in adding a self-enhanced peptide conjugate, as cellular uptake increases 12-fold.[7]

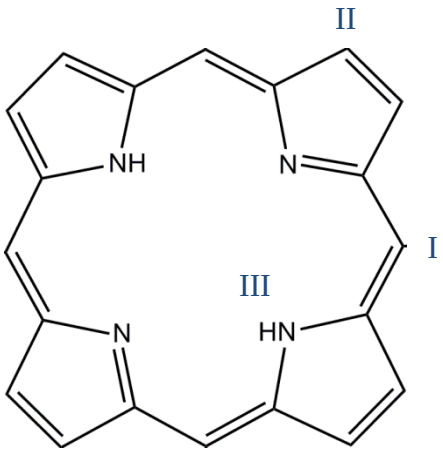

Figure 1.2. Structure of a porphyrin with examples of functionalization sites. I: Meso position, II: β position, III: inner hydrogens

1.4 Carboranes

One of the advantages of BSH is that it utilizes a highly efficient cage structure in which boron comprises a large percentage of the overall mass of the compound.[8] The o-carborane structure is shown below in Figure 1.3 For our purposes, the para orientation will be used rather than the ortho.

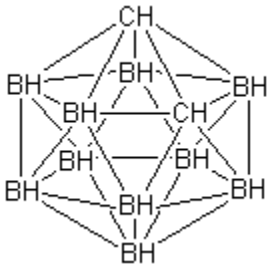

Figure 1.3. Structure of o-carborane

1.5 PDT

PDT is a binary form of cancer therapy in which drug action is locally controlled by light. This technique involves a nontoxic pigment that photosensitizes a compound found in significant quantities in all tissue: oxygen. By converting the normal triplet state oxygen into a singlet state,[9] this process generates cytotoxic reactive oxygen species which causes necrosis of tumorous material. The success of a target PDT drug therefore depends mainly on two biological properties: preferential accumulation into tumor cells, and the localized cytotoxic effect in the presence of light and oxygen.[10]

Treating diseases with light is not a new concept. For example, blue light exposure is used to treat new born babies with neonatal jaundice. PDT uses an Ar laser light for many reasons: it's a high power, high intensity beam and can rapidly switch on and off in order to afford more control in a medical situation.[11,12] Also, while white light contains

lights of many different wavelengths, a laser produces only light of a single wavelength which can be adjusted to suit the required intensity, degree of tissue penetration, composition of the targeted neoplastic material, and, most importantly, the absorption profile of the photosensitizer.

1.6 Current Clinical Trials for PDT

Many compounds are currently in clinical trials for use with PDT. Among them are Photofrin®, an international choice to treat various cancers,[13, 14] Foscan®, used to treat head and neck cancer,[9] and Visudyne®, approved to treat age-related macular degeneration.[15] The main problem with these leading candidates, however, is poor selectivity. This drawback, along with heightened photosensitivity of exposed areas due to slow clearance rate from the body—as long as several weeks[16,17]—draws the eye toward porphyrin candidates.

The ability of porphyrins to selectively accumulate in tumor cells makes it an excellent candidate for a multitude of medical applications.[15] This, along with their photosensitive properties, lends great potential for a PDT candidate.[2,18,19] Unfortunately, their absorption wavelengths are very similar to that of animal tissue—around 416 nm—which can prove problematic in a medical technique that is triggered by light.[20] The photosensitizers of PDT therefore use 620-640 nm light.

1.7 Tetrabenzoporphyrins

Tetrabenzoporphyrins have many of the same qualities outlined earlier in Chapter 1.3. By using a benzo-fused derivation such as tetrabenzoporphyrin (TBP), however, π-conjugation is extended and results in a shift in absorption.[20] Such a porphyrinoid chromophore has an absorption at the near-IR regions, leading to a candidate that is an excellent photosensitizer and minimalizes damage to healthy tissue.

Mono-substituted TBP has already recorded low dark toxicity values, and was determined to be highly phototoxic. With such success for a mono-substituted product, efforts have been focused on synthesizing di-substituted TBP-polyamine conjugates in order to further optimize this candidate.

1.8 Polyamine Conjugates

The abnormal growth of tumor cells surpasses their ability to synthesize them, so the polyamine transport system (PAT) is used to fulfill their needs.[21] Adding a polyamine conjugate to TBP increases tumor selectivity by tapping into its insatiable method of cell growth. The polyamines to be used in the future are in the process of being published, so no specific details will be disclosed. However, they showed great promise during independent *in vitro* studies with PDT because of good cellular uptake.

Cellular uptake should increase with a more hydrophilic compound. So although both di-substituted isomers will be studied, the one with adjacent substituents—and a greater dipole moment—will most likely show greater cellular uptake. Also, as a pleasant side

effect, the introduction of polyamine substituents also increases solubility of TBP in organic solvents.

Ch. 2: Experimental Methods

2.1 Specifications

Reactants and solvents identified as stock solutions were used without further purification and purchased from either Sigma Aldrich or Fischer Scientific. Sensitive reactions were carried out under argon atmosphere in oven-dried glassware. Each reaction was tentatively confirmed using thin layer chromatography (TLC) via 0.25 mm silica gel plates from Sorbent technologies before progressing to the next step in the synthetic scheme. This also served as an indication of which fractions needed to be isolated, and which solvent systems would be most effective when purifying via column chromatography. These purifications were performed using silica gel or Al_2O_3 Grade III gel, both from Sorbent Technologies. When applicable, the reactions were additionally confirmed qualitatively at the formation of each new product with a UV indicator (60F-254). A Bruker DPX-250 spectrometer was used to obtain the ^{1}H-NMR spectra and the reported chemical shifts are all given in ppm relative to $CDCl_3$. A Bruker OmniFLEX MALDI-TOF mass spectrometer was used to obtain mass spectra.

2.2 BNCT

Each step of the synthetic scheme was performed twice: once on a small-scale to qualitatively confirm synthesis of the desired product, and another as a large-scale reaction to synthesize enough of each product to run multiple quantitative tests such as UV-Vis and ^{1}H-NMR. Numbers reported are therefore indicative of the large scale reaction.

2.3 Synthesizing Fluorinated Tetraphenylporphyrin, $TPPF_{20}$ [3]

Pyrrole (1700 mg, 25.3 mmol) [**1**] and pentafluorobenzaldehyde (5000 mg, 25.5 mmol) [**2**] were reacted with a BF_3 and OEt_3 mixture (362 mg, 2.55 mmol) in dry DCM (1.5 L) at room temperature for twenty hours, and were refluxed with DDQ (5700 mg, 25.1 mmol) for two hours. $TPPF_{20}$ [**3**] was then obtained after purification via silica gel column chromatography using a solution of chloroform-hexanes 7:3 for elution to give 3311 mg (56% yield). UV-Vis (DMSO) λ_{max} ($\varepsilon/M^{-1}cm^{-1}$) 413 (426, 389). ^{1}H-NMR ($CDCl_3$, 400MHz) δ 8.95 (8H, s), -2.88 (2H, s).

2.4 Synthesizing $TPPF_{19}OC_3H_3$ [4]

Propargyl alcohol (0.049 mL, 0.83 mmol), anhydrous K_2CO_3 (2810.8 mg, 20 mmol), and acetone (200 mL) were refluxed for 15 minutes. Porphyrin **3** (2441.9 mg, 25 mmol) was added to this mixture and refluxed overnight. Porphyrin **4** was then obtained after purification via silica gel column chromatography using a solution of petroleum ether-chloroform 3:1 elution to give 35 mg (15% yield). UV-Vis (DMSO) λ_{max} ($\varepsilon/M^{-1}cm^{-1}$) 413 (426, 392). ^{1}H-NMR ($CDCl_3$, 400MHz) δ 8.94 (8H, d), 5.24 (2H, s), 2.86 (1H, s), -2.91 (2H, s).

2.5 Synthesizing Zn-metalloporphyrin with carborane substituents [5]

Thiol carborane (26.33 mg, 0.16 mmol), porphyrin **4** (35 mg, 0.04 mmol), and K_2CO_3 (33 mg, 0.24 mmol) in DMF were stirred together at room temperature for 48 hours. The mixture was then dissolved in ethyl acetate and dried using Na_2SO_4 and the residue after evaporation was washed in a brine solution and purified via silica gel column

chromatography using a solution of petroleum ether-chloroform 1:1 elution to give 37 mg (89% yield). For the second part of this reaction, saturated $Zn(OAc)_2$ dissolved in methanol was added in excess to the now-purified dark purple-brown mixture and stirred at room temperature overnight. The exact mass of the $Zn(OAc)_2$/methanol mixture was not measured, though about as much of the mixture was added as the already purified porphyrin without the metal center. This was then dissolved in water and DCM and the bright pink organic layer was isolated via separatory funnel to give 39 mg (98% yield). UV-Vis (DMSO) λ_{max} ($\varepsilon/M^{-1}cm^{-1}$) 422 (411, 431). ^{1}H-NMR ($CDCl_3$, 400MHz) δ 8.99 (8H, q), 5.21 (2H, s), 3.46 (34H, br m).

2.6 Synthesizing Butanopyrrole [8]

Compound **7** (4.1820 g) was heated at 100 °C under Ar with an excess of NaOH (6.0 g, 150 mmol) in ethylene glycol (150 mL) for 30 min, then temperature was increased to 195 °C/30 min. The mixture was allowed to cool to about 80-90 °C, then it was cooled in an ice bath. CH_2Cl_2 (200 mL) was added and the mixture washed with brine (3 x 200 mL). The aqueous phase was washed with CH_2Cl_2 (3 x 100 mL). The combined organic phase was washed with brine (200 mL), dried over Na_2SO_4, and the solvent evaporated under vacuum. The resulting material was purified on a short plug of silica gel using CH_2Cl_2 as eluent to obtain white crystals of butanopyrrole and qualitatively characterized as a bright orange band using a UV indicator [**8**]. Yield of **8**: 2.4660 g (94%).

2.7 Synthesizing Cu-TBP pre-cursor [11-15]

Methyl 4-formylbenzoate [**10**] (1.692 g, 10.3 mmol) and butanopyrrole [**8**] (2.466 g, 20.6 mmol) were dissolved in freshly distilled CH_2Cl_2. Ar was bubbled into the solution for 15 minutes. Five minutes into the bubbling procedure, benzaldehyde [**9**] (1.095 g, 10.3 mmol) was added. After the full 15 minutes, a 2.5 M solution of in BF_3OEt_2 (0.420 g, 0.309 mmol) was prepared under Ar and added to the mixture. The stirring was continued overnight at room temperature. DDQ (8.555 g, 30.9 mmol) was added and the reaction mixture stirred overnight again at room temperature. The solvent was removed under vacuum to leave a purple residue. The residue was dissolved in $CHCl_3$ and filtered through a plug of Al_2O_3 grade III, using $CHCl_3$ as eluent, followed by $CHCl_3$: MeOH 9:5, and $CHCl_3$: MeOH 9:1 mixture.

The filtrate was evaporated under vacuum to leave a purple residue. The purple residue (5 g) was dissolved in toluene (300 mL). To this solution was added anhydrous $CuCl_2$ (10 g) and the reaction mixture refluxed overnight. The solvent was evaporated under vacuum. The product was then dissolved in CH_2Cl_2 and passed through a celite cake. The resulting green solid residue was separated by flash chromatography on silica gel using CH_2Cl_2 : Hexanes 1:1 followed by EtOAc after the second band eluted. Fractions were taken of this product in order to isolate the dimer from its mono-, tri-, and tetra-counterparts via column chromatography with a CH_2Cl_2 : Hexanes 1:2, then 1:1 solvent system.

2.8 Isolating Di-substituted Cu-TBP pre-cursor [12, 13]

The Cu-TBP dimer fraction was isolated and identified, as well as the non-substituted TBP dimer fraction. Both fractions were combined (2 g) and evaporated under vacuum. The previous Cu addition step was then repeated. Granulated fractions were dissolved in 200 mL toluene. To this solution, anhydrous $CuCl_2$ (4 g) was added and the mixture refluxed overnight. The solvent was evaporated under vacuum, dissolved with CH_2Cl_2, and passed through a celite cake. The additional flash chromatography step was omitted. Yield of **12** and **13**: 0.4040 g (8 %). HRMS (MALDI-TOF) calculated for $C_{64}H_{56}N_4O_4$ = 944.234.

2.9 Synthesis of Di-substituted Cu-TBP [16, 17]

Cu-tetrabenzoporphyrin (0.404 g) and DDQ (0.930 g, 3.364 mmol) were dissolved in 70 mL anhydrous toluene under Ar and refluxed for 1 h. The reaction mixture was cooled to room temperature, diluted with $CHCl_3$, washed with saturated $NaHCO_3$ (2 x 200 mL) and water (2 x 200 mL), dried under Na_2SO_4, filtered, and the solvent evaporated under vacuum. The desired product was separated by flash chromatography on silica gel using $CHCl_3$ as eluent giving 0.3815 g (96% yield). HRMS (MALDI-TOF) *m/z* 991.330 [M], calculated for $C_{64}H_{40}CuN_4O_4$ = 991.2340.

Ch. 3: Results and Discussion

3.1 Synthesis of Fluorinated Tetraphenylporphyrin $TPPF_{20}$ [3]

Shown in Schemes 1 and 2 below is the complete synthesis[3, 22, 23, 24] of the desired fluorinated carborane-porphyrin from commercially available pyrrole and pentafluorobenzaldehyde. The synthesis of porphyrin **3** uses the Lindsey method.

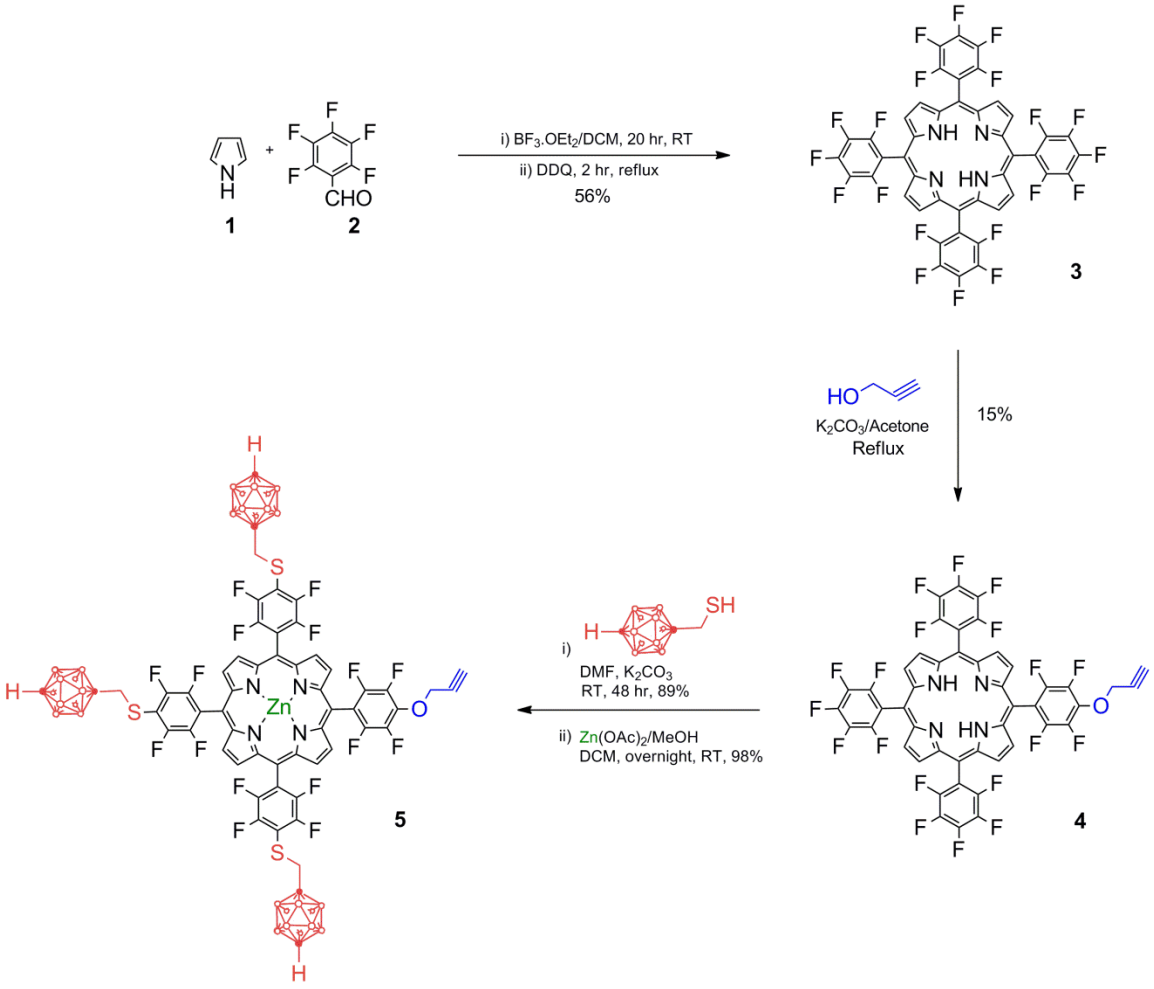

Scheme 1

3.2 Synthesis of $TPPF_{19}OC_3H_3$ [4]

The synthesis of porphyrin **4** involves perform nucleophilic aromatic substitution of a fluorine substituent in order to prepare the mono-substituted porphyrin for peptide conjugation. A low yield is to be expected since this reaction forms the di-, tri-, and tetra-substituted products as well. Most of the yield is lost by isolating the desired mono-substituted product from this mixture. However, the literature reports an 86% yield for this compound. In an effort to maximize our own yield, the Cavaleiro research group at the University of Aveiro was contacted in order to figure out the difference in their techniques. On average, their group was only able to achieve a 15-20 % yield. The 86% yield was a singular event that they were not able to reproduce, nor explain the cause for such an effect.

3.3 Synthesis of Zn-metalloporphyrin with carborane substituents [5]

After the addition of the thiol carborane substituents, zinc is added to the center of this porphyrin in order to stabilize the ring structure before the peptide conjugate is added.

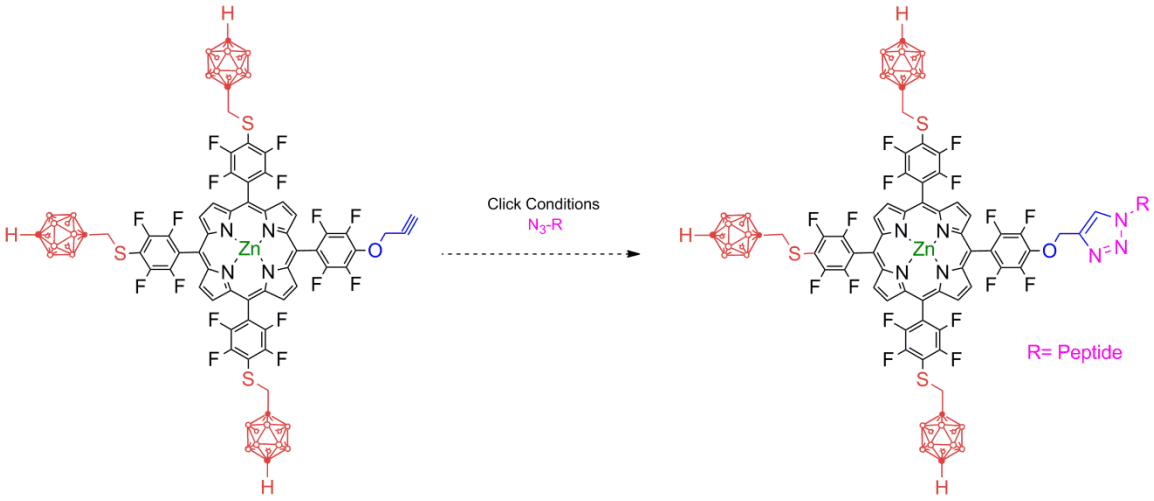

5 **6**

Scheme 2

Dissolving the compound allowed the separation of the unreacted, excess zinc acetate present in a pink layer with the separatory funnel.

3.4 Projected Addition of Peptide Conjugate

The dotted line shown in Scheme 2 indicates a step in the synthesis which has not yet been completed in which a peptide conjugate has been added to porphyrin **5** to produce porphyrin **6**, ready for cytotoxicity and cellular uptake characterizations. This reaction would occur under "Click conditions," in which copper sulfate and ascorbic acids would be used as a catalyst.[25]

3.5 UV-Vis Characterizations for 3, 4, and 5

The UV-Vis trends for all three porphyrins are compared in Figure 3.1 below. As stated in Chapter 1.3, porphyrins show a characteristic red-shifted Soret band, typically at approximately 416 nm. This is most likely due to the formation of a metalloporphyrin with a closed-shell metal ion such as Zn(II). The addition of a metal center in a porphyrin ring should result in very little difference of the Soret peak when compared to its previous porphyrin ring structure, since the d (π) orbitals are relatively low in energy.

The less obvious Q bands show a greater change for the metalloporphyrin when compared to its previous porphyrin structure. For porphyrin rings, four Q bands should be seen. Only two large bands are shown for **3** and **4**, though if the spectra were extended until around 700 nm, the others would most likely be shown. However, this spectra still shows us the trend of how Q bands in metalloporphyrins differ by showing only one large

Q band for **5**. Due to the higher tetragonal (D_{4h}) symmetry of the metalloporphyrin, the 4 Q bands should essentially collapse into two Q bands.[6] Although the figure below shows a 2:1 relationship rather than a 4:2 relationship, we still see the same trend as expected. Therefore, the subtle differences in UV-Vis spectra between **5** compared to **3** and **4** are due to the insertion of Zn into the center of the porphyrin complex.

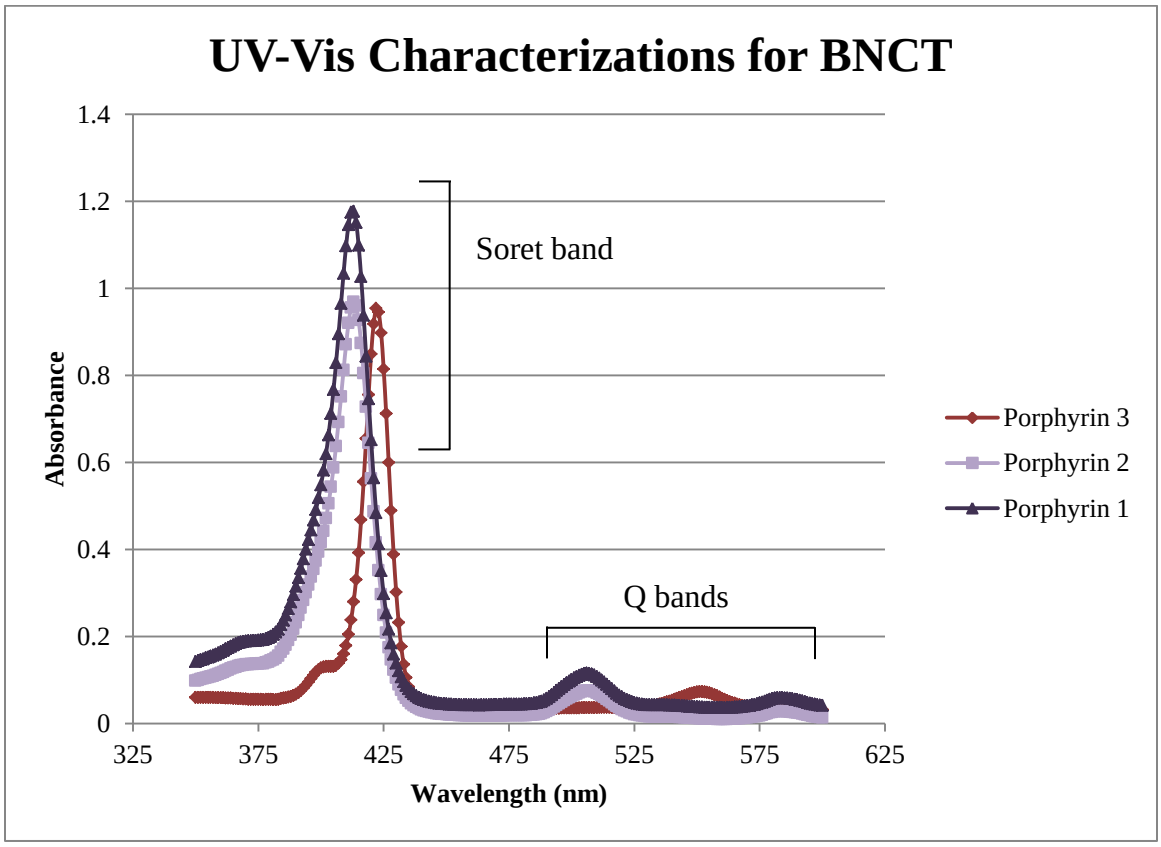

Fig. 3.1 UV-Vis characterizations for Porphyrins 1, 2, and 3, as identified by the legend on the right.

3.6 ^{1}H-NMR Characterizations for 3, 4, and 5

A large peak appeared on each of the spectra which were later identified as acetone (δ 2.03) that remained from recently cleaning the tubes. If the compounds could be run again, the spectra would most likely show the peaks for the porphyrin structure without

this large impurity. However, the characteristic peaks we are looking for on **3** and **4**—at 8 ppm and -2.5 ppm—are clearly visible, confirming the presence of the 8 protons on the outer edges and the two protons on the inner core of the porphyrin structure. The interesting negative peaks on these spectra are due to the heavy shielding those two hydrogens experience by being on the inside of the aromatic ring. Notice that on **5**, in which the two inner hydrogens are replaced with Zn, does not have the -2.5 peak. **5** does, however, have thirty-three additional hydrogens, from the 3 bonded carborane structures. In **4** and **5**, the two peaks at 5.24 ppm and 5.21 respectively agree with the expected literature value 5.23 ppm,[23] which coordinates to the —OCH_2— group of the compound shown in blue. The 2.86 ppm peak for **4** agrees with the expected literature value 2.82 ppm[23] and corresponds to the —C≡CH group. There should be a peak at this value again for **5**, but the peak is very short (as seen in the spectra of **4**) and is not discernible amid the broad multiplet of peaks between 3.46 and 2.03 ppm. However, an extra proton is accounted for amid those peaks, which corresponds to the —C≡CH group in **5**.

3.7 Synthesis and Characterization of Butanopyrrole [8]

Based on past experiments, the pyrrole ester shown below in Fig. 2.3 was readily available. By performing a simple base hydrolysis of an ester, the butanopyrrole component was synthesized.[21,26,27,28] The formation of butanopyrrole was confirmed by the presence of an orange band under long λ UV light.

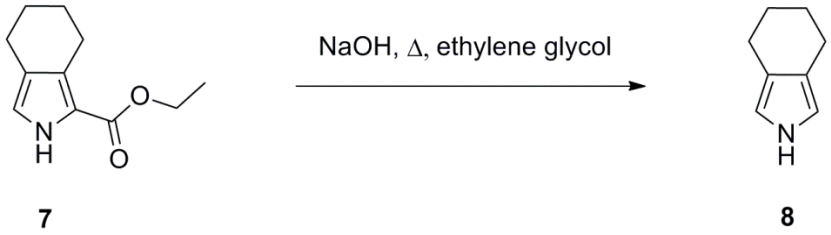

7 **8**

Scheme 3

3.8 Synthesis and Characterization of Di-substituted Cu-TBP pre-cursor [12, 13]

Scheme 4 incorporates the standard Lindsey method to prepare the TBP pre-cursor[26] with a Cu metal center. In performing Synthetic Scheme 2, we modified previous literature procedure and added equal parts benzaldehyde and methyl-4-benzoate in order to maximize the amount of di-substituted product compared to the other mono-, tri-, and tetra- versions. The net ratio of reagents for this reactions was therefore 4:2:2 of butanopyrrole:benzaldehyde:methyl-4-benzoate. During the initial addition of these reagents, we again modified literature procedure by performing two separate additions during the overnight reflux: we added (1) butanopyrrole and methyl-4-benzoate to the RBF as soon as the Ar bubbling began and then (2) added the benzaldehyde five minutes later. A seemingly small adjustment, but it allowed for a slower, more thorough mixture. Had all the reagents been added at once, the mixture would have turned purple immediately. As it is, the mixture remained a golden yellow color until turning purple a few hours later.

Before purifying the desired product, a TLC plate was performed, but we weren't able to clearly distinguish the desired band. We therefore isolated and discarded the band of

unreacted DDQ as identified by column chromatography and inserted the copper metal center into the ring; the di-substituted compound was easier to determine in this extremely stable structure. We were able to gather and identify fractions from column chromatography and tentative MALDI-TOF mass spectra of 3 separate bands of interest: the mono-substituted compound, a mono- and di-substituted mixture, and the di-substituted compound. There were many additional impurities present when this spectra was taken, but the readings were helpful in identifying the relationship among each set of bands. The mixture was separated through column chromatography again in order to maximize the yield of the di-substituted compound. Upon an additional MALDI reading, we determined that the di-substituted product was composed of a mixture of di-substituted porphyrin ring and di-substituted metalloporphyrin. The copper addition step was therefore repeated. Even with this additional step, we were only able to produce a low yield with a large amount of impurities.

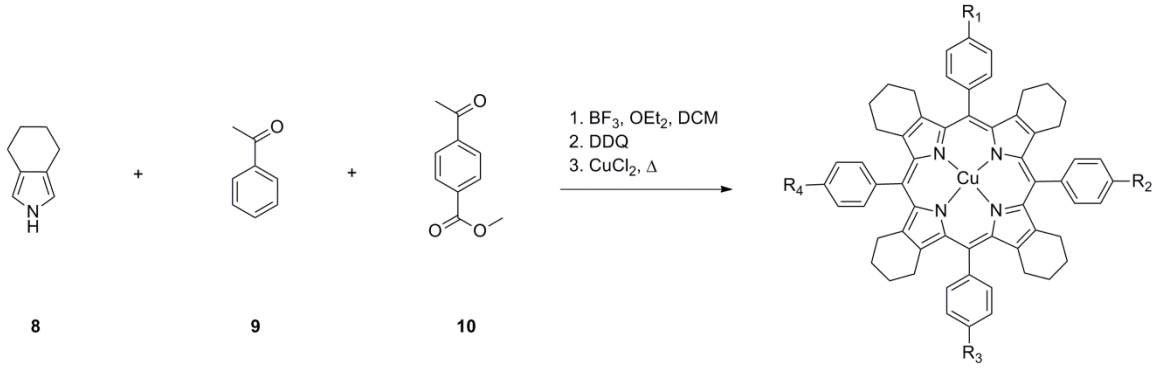

11: $R_1 = CO_2Me$; $R_2 = R_3 = R_4 = H$
12: $R_1 = R_2 = CO_2Me$; $R_3 = R_4 = H$
13: $R_1 = R_3 = CO_2Me$; $R_2 = R_4 = H$
14: $R_1 = R_2 = R_3 = CO_2Me$; $R_4 = H$
15: $R_1 = R_2 = R_3 = R_4 = CO_2Me$

Scheme 4

3.9 Synthesis and Characterization of Di-substituted Cu-TBP [16, 17]

This synthetic step features a series of modularized porphyrins in which the TBP-precursor becomes a fully-fledged benzo-fused compound. From this, we are able to modify the substituents to prepare for the addition of polyamine conjugates. The MALDI characterization according to literature[25] was slightly closer than our own at 991.2325 and 991.2340. Many attempts were made to isolate the di-substituted compounds from each other, both through TLC and column chromatography. This would be the ideal point in which to separate these two isomers because the next step involves deprotecting the ring by removing the Cu metal from the center of the porphyrin ring and decreasing the overall stability of the structure. In addition, x-ray crystal diffraction should be used in order to identify the orientation of each regio-isomer; the methylated product at this step is much easier to crystallize than the TBP—COOH would be in the upcoming step. It is potentially possible to separate the isomers from each other using large plate chromatography (a large scale version of TLC), although both TLC and column chromatography are not able to provide clearly distinguishable bands with the impurities and the continued attempts to separate them had begun to take a significant toll on the net amount of product. An alternative synthetic method was therefore begun in order to maximize yield of the di-substituted compound and continue the attempts to separate them, with a zinc metalloporphyrin. The focus has therefore shifted to the optimization of reaction conditions, currently underway.

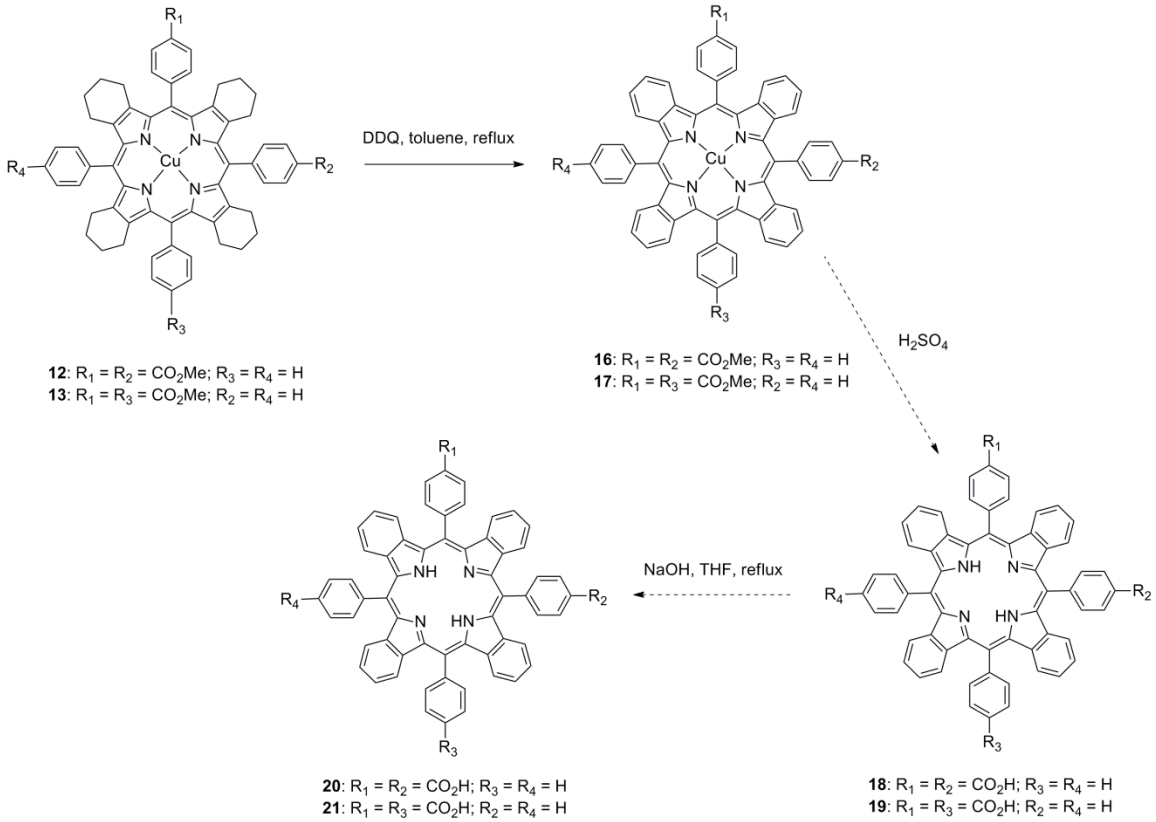
DDQ, toluene, reflux
H2SO4
NaOH, THF, reflux
12: R1 = R2 = CO2Me; R3 = R4 = H
13: R1 = R3 = CO2Me; R2 = R4 = H
16: R1 = R2 = CO2Me; R3 = R4 = H
17: R1 = R3 = CO2Me; R2 = R4 = H
18: R1 = R2 = CO2H; R3 = R4 = H
19: R1 = R3 = CO2H; R2 = R4 = H
20: R1 = R2 = CO2H; R3 = R4 = H
21: R1 = R3 = CO2H; R2 = R4 = H

Scheme 5

Ch. 4: Conclusions

Synthesis of **3**, **4** and **5** were all successful, as shown by their UV-Vis and ^{1}H-NMR characterizations. In the future, further chemical and biological characterizations, including quantifying toxicity levels to determine the integrity of the final carborane-porphyrin product, could be performed in order to determine the quality of this compound as a viable candidate if a suitable peptide conjugate were identified and added under Click conditions.

The desired synthetic scheme for the PDT candidate until the Cu-tetrabenzoporphyrin with di-substituted ester constituents [**16**, **17**] was successfully synthesized, as shown by HRMS characterization. The purpose of this synthesis was to test the toxicity and cellular uptake of the tetrabenzoporphyrin with di-substituted polyamine conjugates because the previous mono-substituted TBP produced such promising results. Since the separation of one di-substituted compound from the other has been such a long-standing problem, a more fruitful solution might be to instead synthesize and test the tetra-substituted compound with adjusted Scheme 4 reagent ratios, doing away with the separation of di-substituted (or even tri-substituted) compounds altogether. If favorable results are determined, the next step would be to investigate maximizing the yield of the tetra-substituted compound through further additions. From a practical standpoint, it is important that a drug be synthesized that is not only an excellent candidate for this therapeutic technique, but is also feasibly synthesized on a large, mass-producible scale.

References

1. Hawthorne, M. F.; *Agnew. Chem. Int. Ed. Engl.* **1993**, *32*, 950.

2. Soloway, A. H.; Tjarks, W.; Barnum, B. A.; Rong, F. G.; Barth, R. F.; Codogni, I. M.; Wilson, J. G.; The Chemistry of Neutron Capture Therapy. *Chem Rev* **1998,** *98* (4), 1515-1562

3. Barth, R. F.; Coderre, J. A.; Vicente, M. G. H.; Blue, T. E.; Boron Neutron Capture Therapy of Cancer: Current Status and Future Prospects. *Clinical Cancer Research* **2005**, *11*, 3987-4002.

4. Behr, T.; Béhé, M.; Stabin, M.; Wehrmann, E.; Apostolidis, C.; Molinet, R.; Strutz, F.; Fayyazi, A.; Wieland, E.; Gratz, S.; Koch, L.; Goldenberg, D.; Becker, W.; High-Linear Energy Transfer (LET) α *versus*Low-LET β Emitters in Radioimmunotherapy of Solid Tumors: Therapeutic Efficacy and Dose-limiting Toxicity of ^{213}Bi- *versus*^{90}Y-labeled CO17-1A Fab′ Fragments in a Human Colonic Cancer Model. *Cancer Res.* 1999, *59*, 2635.

5. Gottumukkala, Vijay. Ph. D. Dissertation. Louisiana State University, 2006.

6. Huange, X.; Nakanishi, K.; Berova, N.; Porphyrins and Metalloporphyrins: Versatile Circular Dichroic Reporter Groups for Structural Studies. *Chirality.* 2000. **23**: 237-255.

7. M. Sibrian-Vazquez, E. Hao, T. J. Jensen and M. G. H. Vicente. Enhanced Cellular Uptake with a Cobaltacarborane-Porphyrin-HIV-1 Tat 48-60 Conjugate. *Bioconjugate Chemistry* 2006. **17:** 928-934

8. Hao, E.; Friso, E.; Miotto, G.; Jori, G.; Soncin, M.; Fabris, C.; Sibrian-Vazquez, M.; Vicente, M.G.H. *Org. Biomol. Chem.* 2008. **6**: 3732.

9. Sol, V.; Lamarche, F.; Enache, M.; Garcia, G.; Granet, R.; Guilloton, M.; Blais, J. C.; Krausz, P.; Polyamine conjugates of meso-tritolylporphyrin and protoporphyrin IX: Potential agents for photodynamic therapy of cancers. *Bioorganic & Medicinal Chemistry* 2006, *14* (5), 1364-1377.

10. Songca, S. P., In-vitro activity and tissue distribution of new fluorinated meso-tetrahydroxyphenylporphyrin photosensitizers. *Journal of Pharmacy and Pharmacology* 2001, *53* (11), 1469-1475.

11. Astruc, D.; Boisellier, E.; Ornelas, C. T.; Dendrimers Designed for Functions: From Physical, Photophysical, and Supramolecular Properties to Applications in Sensing, Catalysis, Molecular Electronics, Photonics, and Nanomedicine. *Chem Rev* **2010,** *110* (4), 1857-1959.

12. Drain, C. M. Varotto, A.; Radivojevie, I.; Self-Organized Porphyrinic Materials. *Chem Rev* **2009,** *109* (5), 1630-1658.

13. Ascencioa, M. Delemera, M. Farineb, M. O. Jouvea, E. Collineta, P. Mordon, S. Evaluation of ALA-PDT of ovarian cancer in the Fischer 344 rat tumor model. Photodiagnosis and Photodynamic Therapy (2007) 4, 254-260.

14. Weimin, S.; Gen, Z.; Guifu, D.; Yunxiao, Z.; Jin, Z.; Jingchao, T., Synthesis and in vitro PDT activity of miscellaneous porphyrins with amino acid and uracil. *Bioorganic & Medicinal Chemistry* **2008,** *16* (10), 5665-5671.

15. Vicente, M. G., Porphyrin-based sensitizers in the detection and treatment of cancer: recent progress. *Curr Med Chem Anticancer Agents* **2001,** *1* (2), 175-94.

16. Garcia, G.; Sarrazy, V.; Sol, V.; Morvan, C. L.; Granet, R.; Alves, S.; Krausz, P., DNA photocleavage by porphyrin-polyamine conjugates. *Bioorganic & Medicinal Chemistry* **2009,** *17* (2), 767-776

17. Chaleix, V.; Sol, V.; Guilloton, M.; Granet, R.; Krausz, P., Efficient synthesis of RGD-containing cyclic peptide-porphyrin conjugates by ring-closing metathesis on solid support. *Tetrahedron Letters* **2004,** *45* (27), 5295-5299.

18. Hao, E.; Jensen, T. J.; Courtney, B. H.; Vicente, M. G. H.; Synthesis and Cellular Studies of Porphyrin-Cobaltacarborane Conjugates. *Bioconjugate Chemistry* **2005,** *16* (6), 1495-1502

19. Sibrian-Vazquez, M.; Nesterova, I. V.; Jensen, T. J.; Vicente, M. G. H., Mitochondria Targeting by Guanidine— and Biguanidine—Porphyrin Photosensitizers. *Bioconjugate Chemistry* **2008,** *19* (3), 705-713.

20. Kadish, K. M.; Smith, K. M.; Guilard, R., *The porphyrin handbook.* Academic Press: San Diego, 2000.

21. Amuhaya, Edith. Ph. D. Dissertation. Louisiana State University, 2011.

22. Volz, H; Schneckenburger, S. *J. prakt. Chem.* 1993. **335**: 283.

23. Santos F.C.; Cunha, A. C.; de Souza, M. C. B. V.; Tome, A. C.; Neves, M. G. P. M. S.; Ferreria, V. F.; Cavaleiro, J. A. S. *Tetrahedron Lett*. 2008. **49**: 7268.

24. Ujvary, F.; Nachman, R.J. *Tetrahedron Lett.* 1999. **40**: 5147.

25. Rostovtsev, V. V.; Green, L. G.; Fokin, V. V.; Sharpless, K. B.; *Angew. Chem.* **2002**, *114*, 2708-2711; *Angew. Chem., Int. Ed.* **2001**, *40*, 2004-2021.

26. Filatov, M. A.; Cheprakov, A. V.; Beletskaya, I. P., A Facile and Reliable Method for the Synthesis of Tetrabenzoporphyrin from 4,7-Dihydroisoindole. *European Journal of Organic Chemistry* **2007,** *2007* (21), 3468-3475.

27. Vogler, A.; Kunkely, H., Simple Template Synthesis of Zinc Tetrabenzoporphyrin. *Angewandte Chemie International Edition in English* 1978, *17* (10), 760-760.

28. Remy, D. E., A versatile synthesis of tetrabenzoporphyrins. *Tetrahedron Letters* 1983, *24* (14), 145101454.